Photo-Sensor Characteristics for a Multi-PMT Optical Module in KM3NeT

O. Kavatsyuk[*], Q. Dorosti-Hasankiadeh[*] G. Inguglia[*], and H. Löhner[*]
representing the KM3NeT Consortium

[*] *KVI, University of Groningen, Zernikelaan 25, 9747 AA Groningen, The Netherlands*

***Abstract*. An efficient search for high-energy (1-1000 TeV) neutrinos originating from galactic and extragalactic sources requires a km^3 sized deep sea Neutrino Telescope. An optical module containing an array of 31 small photo-multiplier tubes is a promising alternative to an optical module containing a 10-inch diameter phototube. A suitable 3-inch diameter phototube has been selected and further developed in gain performance, with a cathode window matched to the curvature of the glass pressure sphere of the optical module. The properties of single phototube samples have been investigated with emphasis on high quantum efficiency at low dark noise. A voltage-divider circuit with a built-in preamplifier allows for reducing heat dissipation, electronic noise and dark current. The operation of tubes at a gain of 10^6 provides a good peak-to-valley ratio of about four. A remote-controlled 2D scanning system allows for precise measurements of the photocathode homogeneity and sensitivity with respect to position and angle of incidence. The measured characteristics of the Photonis XP53B20 phototubes are presented and the perspectives for their integration into a Multi-PMT optical module for the future KM3NeT detector are discussed.**

***Keywords*: KM3NeT, neutrino telescope, optical module, position sensitivity**

I. Introduction

The ANTARES [1] underwater neutrino telescope, fully operational since May 2008, covers an effective area of ≈0.05 km^2 and aims at the detection of upgoing muon tracks generated by high energy neutrinos having passed through the Earth. Although being the largest neutrino detector viewing the Galactic Centre, an efficient search for high-energy (1-1000 TeV) neutrinos originating from galactic and extra-galactic sources requires a km^3 sized deep sea Neutrino Telescope (KM3NeT)[2] which is currently being developed. Based on the experience gained in the Mediterranean pilot projects ANTARES [1], NEMO [3] and NESTOR [4], the KM3NeT consortium has developed the concept for a large deep-sea infrastructure [5]. The detection principle exploits the measurement of Cherenkov light emitted by charged secondary particles resulting from neutrino interactions in the matter surrounding the telescope. Accurate measurements of the light arrival

Fig. 1. Prototype of the MultiPMT optical module

times and amplitudes are required. These, together with a precise knowledge in real time of the positions and orientations of the photo-sensors, are mandatory to reconstruct direction and energy of the neutrinos with an angular resolution better than 0.3° above a few TeV, necessary to identify possible discrete neutrino sources. In order to improve the rejection of environmental background and to increase the sensitivity to ultra-high energy neutrinos, a new optical module (OM) with an arrangement of several small photo-multiplier tubes (PMTs) is considered as a possible solution in the KM3NeT Conceptual Design Report [5] and a prototype OM is being developed by the KM3NeT consortium. The sensitive photocathode area of 31 phototubes of 3-inch type is about 15% larger [5] than that of three Hamamatsu R7081-20 tubes as currently employed in ANTARES. The advantages of multiple small PMTs in the same OM are the tesselated directional sensitivity (Fig. 1), high quantum efficiency (QE>30%) for standard bi-alkali and possibly even higher for super-bialkali tubes, smaller transit time spread and better two-photon separation capability [7]. Moreover, at the same gain the accumulated charge on small tubes is smaller than for large PMT which implies a longer lifetime than expected for large PMT. In addition, small PMTs are insensitive to the Earth's magnetic field and do not require μ-metal shielding. Since handling the data flow from the large

Fig. 2. The tested Photonis XP53B20 PMT.

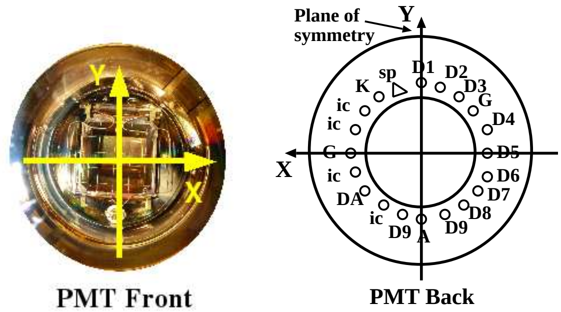

Fig. 3. Coordinate system used for photocathode scan. See text for details.

number of PMT in such an OM solution becomes more challenging, a cost-efficient readout system is being developed [5], [6] with complete digitization inside the OM. Also the reliability of the MultiPMT OM is higher, since failure of single PMT will have much less influence on the performance of the total OM. The above mentioned advantages of the new OM design could significantly improve the reconstruction of neutrino events in KM3NeT. First result from the Monte Carlo simulations including the MultiPMT OMs will be presented in a separate contribution to this conference [8].

II. INSTRUMENTATION

A. PMT Photonis XP53B20

A suitable 3-inch diameter PMT (Photonis XP53B20) has been selected and further developed in gain performance, with a convex-shaped cathode window matched to the curvature of the glass sphere of the optical module (Fig. 2). The Photonis XP53B20 tube has an improved bi-alkali photocathode with spectral range of 290–700 nm and maximum sensitivity at 440 nm. A compact box-and-grid structured 10-stage electron multiplier allows a short tube design required for a compact MultiPMT OM. The PMT glass cylinder is covered with conductive paint at cathode potential to reduce ion-feedback. A PMT base with a built-in preamplifier, designed at Nikhef, was installed in order to reduce heat dissipation, electronic noise and dark current.

B. Test bench

The properties of single PMT samples have been investigated with emphasis on high QE at low dark noise. For testing purposes single PMTs were placed inside a light tight box (DarkBox) with temperature monitors on the cathode entrance window and PMT-base. A PMT was placed inside a cylindrical holder with a Kapton foil for additional electrical insulation. As a light source a light emitting diode (LED) driven by a pulser [9] developed for the ANTARES optical module was used. A trigger output form the LED pulser was used as a start signal for the data acquisition. The light from the LED was guided with a light-fibre inside the DarkBox and shone onto the centre of the PMT perpendicular to the entrance window. The light fibre had a diameter of 0.6 mm and numerical aperture of 0.4. In order to achieve a smaller spot size and collimated beam, a brass collimator was added. This setup allowed an opening angle of 2° and a spot size of 1.4 mm at the centre of the entrance window with a distance of 3 mm from the fibre to the PMT. Signal shapes were recorded by a fast sampling ADC (Acqiris DC282) with a sampling rate up to 8 GHz and a direct current accuracy of 2%.

A remote-controlled 2D scanning system placed inside the DarkBox allowed precise measurements of the photocathode homogeneity and sensitivity with respect to position and angle of incidence. The scanning system consists of two linear stages that allow scanning in horizontal and vertical directions with travel range of 150 and 100 mm, respectively. Additionally, a rotational stage is installed for measurements at different angles of incidence. The stages are equipped with stepper motors providing a repeatability of 1.5 μm. The orientation of a PMT in the setup was defined by the orientation of the dynode structure. The origin of the coordinate system is the centre of the entrance window. The Y axis lies in the plane of symmetry of the electron multiplier chain, perpendicularly to the dynodes. In practice, the correspondence between pin layout and inner configuration was used: the Y axis points from the anode to the first dynode pin (Fig.3).

III. RESULTS

A. SPE spectrum and Dark noise rate

The operation of tubes at a gain of 10^6 provides a good peak-to-valley ratio between four and five for different PMT samples. A typical measured charge spectrum is shown in Fig. 4 (obtained for a PMT with a serial number (SN) 127). The position of the single-photoelectron (SPE) peak was determined and the PMT gain was derived. Fitting Gaussian curves to the measured charge-distribution results in the solid curve containing contributions from 1, 2 and 3 photo electrons (dotted curves). Applying the Poisson distribution the number of photoelectrons per a flash from the LED-pulser was estimated to be 0.46. Figure 5 shows gain

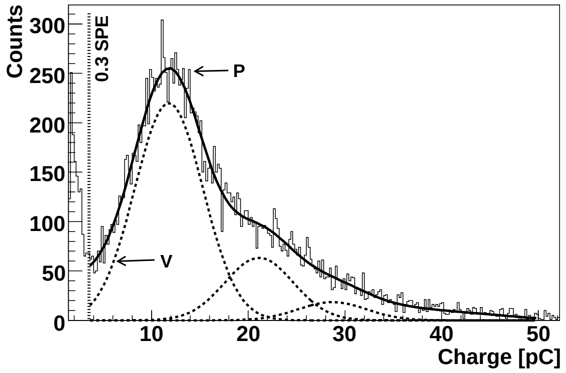

Fig. 4. Measured charge distribution at gain 10^6 for SN127. See text for details.

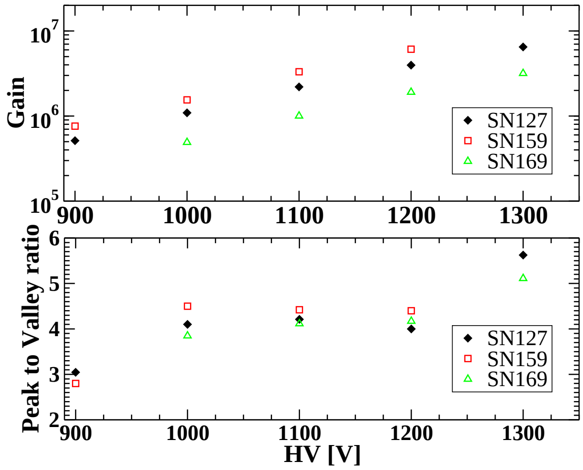

Fig. 5. Gain (*upper part*) and peak-to-valley ratio (*lower part*) as function of the applied high voltage

and peak-to-valley ratio as function of the applied high voltage (HV), in the upper and lower parts, respectively, for three PMT samples available at the time of writing this paper. For more detailed and systematic tests, 40 PMT samples are available now.

In order to determine the dark-noise rate above the 0.3 SPE threshold (indicated by a vertical dotted line in Fig. 4), a constant fraction discriminator (CFD) was used. In order to avoid counting after-pulses, the width of the CFD gate was set to 100 ns. In order to avoid counting after-pulses, the width of the CFD gate was set to 100 ns. A probability of 3% was found for afterpulses beyond 100 ns. The results were confirmed by measuring the charge distribution with a 10 kHz random trigger and determining the integral above 0.3 SPE normalised to the Acqiris live-time. Typical values for the dark current rate (R_{dark}) at a gain of 10^6 and the corresponding dark current (I) are given in Table I. The fourth column of Table I shows values from specification sheets for comparison.

B. The photocathode homogeneity

The effective area of a PMT is defined as an area with a relative collection efficiency of at least 80% relative to

TABLE I
MEASURED DARK COUNT RATE ABOVE 0.3 SPE AT 20°.

PMT	R_{dark} [kHz]	I [nA]	I_{spec} [nA]
SN127	5	0.8	7.5
SN150	25	4.0	15.6
SN157	15	2.4	6.6
SN169	3	0.5	2.3
SN159	15	2.4	10.4

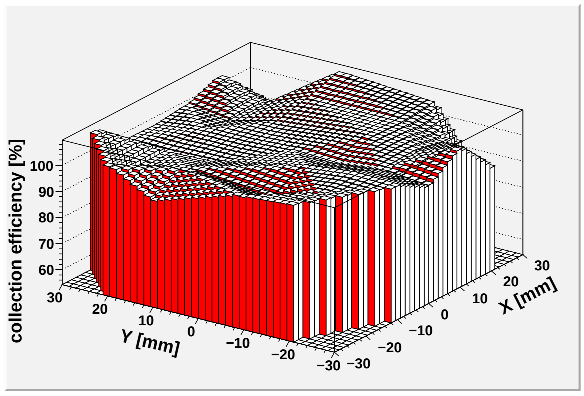

Fig. 6. 2D scan of the photocathode surface

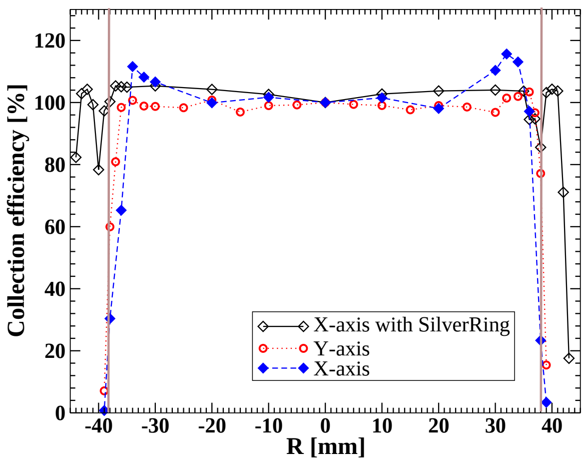

Fig. 7. Relative collection efficiency as a function of the position on the photocathode . Grey vertical lines indicate the contact between the PMT and the Silver Ring. Coordinate system is explained in Fig. 3.

the value at the centre of a photocathode. The obtained 2D scan of the cathode sensitivity is presented in Fig. 6. The relative collection efficiency as a function of the position on the photocathode is shown in Fig. 7. The efficiency is presented for scans over the photocathode along the Y- and X-axes by points shown as filled squares and diamonds, respectively. Figure 3 shows a sketch of the applied coordinate system. Obtained data on the collection efficiency over the photocathode reveal a sensitive photocathode radius of 37±1.6 mm. Uncertainty is mainly caused by the light spot size on the PMT entrance window.

C. PMT with light guiding ring

The dense packing constrains the space available for power supply and readout in the centre of the OM.

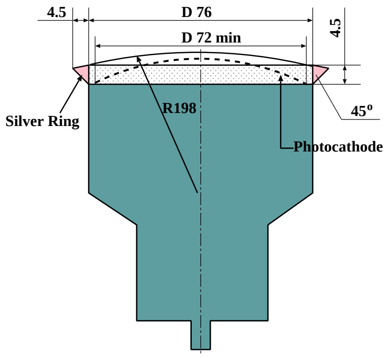

Fig. 8. Sketch of a PMT with a Silver Ring attached to the circumference of the entrance window (Sizes are given in mm).

However, due to the tube design, extra space is available on the inner surface of the sphere, surrounding the cathode entrance window. To exploit this extra space for light collection, a glass or perspex (PMMA) ring may be employed to guide the light to the photocathode.

For the Photonis XP53B20 PMT the convex-shaped glass window has a thickness of 4.5 mm at the circumference, leaving this height available for the entrance of light from the side. A prototype of a 4.5 mm thick ring was manufactured from polished PMMA reflecting light from the side onto the photocathode (Fig. 8). The reflection via a 45 degree tilted surface was improved by silver evaporation (Silver Ring). Application of such a light-reflecting ring increases the sensitive photocathode radius up to 42.5±1.6 mm.

Charge spectra measured with light shining on the ring surface (outside the tube) look very much the same as when shining on the surface of the entrance window of the PMT. In Fig. 7 the relative collection efficiency for PMT SN127 with (empty diamonds) and without the ring (filled diamonds) is presented. Figure 9 shows the peak-to-valley ratio for the same scan (along X-axis) with the Silver Ring as in Fig. 7. The asymmetry in the distribution seems to be a property of the photocathode of this single tube and was confirmed in other measurements.

The collection efficiency from the area outside the photocathode is very high (more than 80% of the value in the centre). The drop in collection efficiency near the optical interface between the Silver Ring and the glass of the PMT (at R = ±38 mm) is probably caused by imperfections in the contact made by optical grease. In the final design we aim to manufacture the entrance window and the ring as one homogeneous unit. By using the Silver Ring the sensitive photocathode area is increased by 32%.

IV. Conclusions

The sensitive photocathode area of the 31 3-inch tubes with 37 mm sensitive radius is about 17% larger and, employing the Silver Ring, even 54% larger than that of three 10-inch tubes as currently employed in ANTARES (with 220 mm cathode diameter given in data sheets).

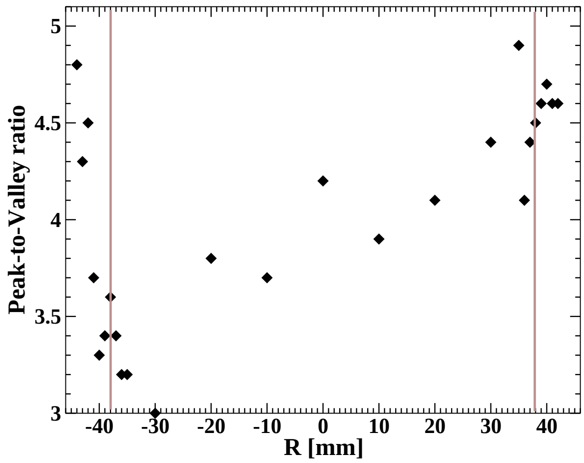

Fig. 9. Peak-to-valley ratio as a function of the photocathode position for SN127 at 10^6 gain. Grey vertical lines indicate the contact between the PMT and the Silver Ring. Coordinate system is explained in Fig. 3

If an expected QE of minimum 35% for 3-inch PMT is considered, as compared to 23% of the 10-inch PMT, this gives another factor of 1.52 in efficient cathode area. All together, a MultiPMT OM with light guiding rings will be about 2 times better in terms of efficient photocathode area. The investigation of QE of the Photonis XP53B20 PMT is the subject of a separate contribution to this conference [10]. More samples will be investigated to confirm the obtained results. The tested PMT type Photonis XP53B20 is a good candidate to be used in the MultiPMT OM. However, dark noise rate needs further improvement. Since the Photonis company is going to stop development and production of PMTs this year, the KM3NeT Consortium is investigating the possibility to use a PMT with comparable characteristics of other producers.

V. Acknowledgements

This work is supported through the EU-funded FP6 KM3NeT Design Study Contract No. 011937.

References

[1] M. Circella, NIM A 602, 1-6 (2009)
[2] U. Katz, NIM A 602, 40-46 (2009)
[3] A. Capone et al., NIM A 602, 47-53 (2009)
[4] P.A. Rapidis, NIM A 602, 54-57 (2009)
[5] P. Bagley et al., 2008, KM3NeT Conceptual Design Report for a Deep-Sea Research Infrastructure in the Mediterranean Sea incorporating a Very Large Volume Neutrino Telescope, ISBN 978-90-6488-031-5; www.km3net.org/CDR/CDR-KM3NeT.pdf
[6] P. Kooijman, contribution to ICRC 2007; P. Kooijman, NIM A 567, 508 (2006)
[7] H. Löhner, A. Mjøs, NIM A 602, 209-212 (2009), doi:10.1016/j.nima.2008.12.037
[8] R. Shanidze, *Event reconstruction in KM3NeT with multi-PMT optical modules*, contribution to this conference
[9] J.S. Kapustinsky et al., NIM A 241, 612 (1985)
[10] B. Herold and O. Kalekin *Characterisation of Photomultiplier Tubes s for KM3NeT*, contribution to this conference